A chemical kinetic study of tetrahydropyran high-pressure oxidation in a jet-stirred reactor

Bakr Hoblos, Zeynep Serinyel, Guillaume Dayma, Philippe Dagaut

Combustion and Flame 268 (2024) 113642

Contents lists available at ScienceDirect

Combustion and Flame

journal homepage: www.sciencedirect.com/journal/combustion-and-flame

A chemical kinetic study of tetrahydropyran high-pressure oxidation in a jet-stirred reactor

Bakr Hoblos [a,b], Zeynep Serinyel [a,b,*], Guillaume Dayma [a,b], Philippe Dagaut [b]

[a] Université d'Orléans, 6 avenue du Parc Floral, 45100, Orléans, France
[b] CNRS–ICARE, 1C avenue de la Recherche Scientifique, 45071 Orléans cedex 2, France

ARTICLE INFO

Keywords:
Biofuel
Tetrahydropyran
Oxidation
Jet-stirred reactor
Kinetic model

ABSTRACT

Cyclic ethers are commonly formed as intermediates during the low-temperature oxidation of hydrocarbons. Tetrahydropyran (THP) is one of the most important cyclic ethers, recently considered as an interesting and promising oxygenated molecule in the context of development of next-generation biofuels. This is essentially due to its substantial existence in the structural core of glucose and many other sugars, which play a crucial role in the oxidation and pyrolysis chemistry of lignocellulosic biomass. In the present work, the oxidation of THP was studied in a jet-stirred reactor. Fuel-lean ($\varphi = 0.5$), stoichiometric ($\varphi = 1$) and fuel-rich ($\varphi = 2$ and 4) mixtures were oxidized at an initial fuel mole fraction of 1000 ppm, a pressure of 10 atm, a residence time of 700 ms, and for temperatures ranging from 480 to 1260 K. Gas chromatography and Fourier transform infrared spectroscopy were used to determine the mole fraction profiles of the different reactant, product and intermediate species. Based on these profiles, a detailed kinetic mechanism for the oxidation of THP was developed in this work. THP exhibits a low-temperature reactivity which becomes less pronounced with the increase of equivalence ratio and almost disappears at $\varphi = 4$. This reactivity is explored for the first time in the present study. Reaction pathway analyses were performed with the developed model and the overall reactivity was found to be primarily driven by the chemistry of the fuel radical adjacent to the ether group. The proposed mechanism generally shows a good performance for representing the present experimental results, as well as other literature data (ignition delay times and plug flow reactor data). However, more data (e.g., atmospheric pressure speciation and laminar flame speeds) are still required for further validation of the present mechanism and to have a better understanding of the kinetic behavior of THP.

1. Introduction

Today most liquid fuels are derived from fossil fuels, and specifically from petroleum. However, due to the high environmental impact of such fuels as well as their accelerated depletion, there has been a growing need to boost the development of clean and renewable alternatives, like biomass-derived products. That's why researchers are currently studying potential biofuels in more detail, especially in terms of their combustion kinetics and the pollutants formed during their oxidation. Due to the oxygen atom characterizing their structure, ethers are considered among the typical model components used to represent oxygenated biofuels. Most previous studies investigating ethers oxidation focused on those with linear chains such as dimethyl [1,2], diethyl [3,4], dipropyl [5,6] and dibutyl [7,8] ethers. Nevertheless, cyclic ethers are not less important in this context. In fact, their role is crucial in understanding the chemistry of both the engine auto-ignition of hydrocarbon fuels and the combustion of oxygenated biofuels as discussed in the two recent comprehensive studies of Rotavera and Taatjes [9] and Tran et al. [10].

Tetrahydropyran (THP) is one of the most important cyclic ethers. It has a promising role in the development of next-generation biofuels, which do not compete with the food production chain. Indeed, this six-membered heterocyclic compound constitutes the structural core of many sugars, including glucose, which appear as key molecules during different conversion processes of lignocellulosic biomass [11,12]. In addition, THP and its derivatives are among the cyclic ethers commonly produced as intermediates during the low-temperature oxidation (cool flame) of some hydrocarbons, and particularly alkanes [13]. Thus, its subsequent reactions may affect the overall reactivity of such hydrocarbons. In accordance with its foregoing characteristics, THP is an interesting species worth being deeply explored and studied.

* Corresponding author at: Université d'Orléans, 6 avenue du Parc Floral, 45100, Orléans, France.
E-mail address: zeynep.serinyel@cnrs-orleans.fr (Z. Serinyel).

https://doi.org/10.1016/j.combustflame.2024.113642
Received 3 June 2024; Received in revised form 23 July 2024; Accepted 28 July 2024
Available online 10 August 2024

The first study on the combustion of THP was published in 1991 by Leppard [14], who used a piston engine to explore the auto-ignition of THP at an equivalence ratio of 0.95 to 1.0, a temperature of 358 K, and a pressure of 60 kPa. Then, in 1997, Dagaut at al. [15] studied the ignition and oxidation of THP in a shock tube and in a jet-stirred reactor (JSR) under a wide range of conditions: a pressure up to 10 atm, an equivalence ratio between 0.5 and 2.0, and a temperature range of 800–1700 K. They also developed a numerical kinetic model to perform simulations for their high-temperature experimental results. Labbe et al. [16] examined the flame chemistry of THP using vacuum-ultraviolet photoionization molecular-beam mass spectrometry and designed a kinetic mechanism for THP flame modeling. Their study was restricted to a laminar premixed flat flame of THP/O_2/Ar mixture at a low pressure of 20 Torr and under a fuel-rich condition ($\varphi = 1.75$). Tran et al. [17] studied both pyrolysis and combustion of THP. They performed pyrolysis experiments using a tubular flow reactor for a constant THP molar flow rate of 1.68×10^{-4} mol.s^{-1} with two different N_2 dilution factors (90 % and 96 %), at a pressure of 170 kPa and a temperature range of 913–1133 K. Then, they conducted combustion experiments in two premixed flat flame burners and in a shock tube. The first burner was operated at a low pressure of 50 Torr with 78 % Ar under two various equivalence ratios (1 and 1.3). The second burner was used to measure the laminar burning velocities of THP/air mixtures using the heat flux method at atmospheric pressure, three different inlet gas temperatures (298, 358 and 398 K) and an equivalence ratio range (0.55 to 1.5). Then, the shock tube was used to measure the ignition delay times of THP/O_2/Ar mixtures under a range of pressures (885–914 kPa), temperatures (1350–1613 K) and equivalence ratios (0.5–2). Finally, the authors developed a detailed kinetic mechanism suitable for the high-temperature oxidation and pyrolysis of THP.

While all the aforementioned studies focused only on the high-temperature reactivity of THP, the low-temperature oxidation of this potential biofuel has recently attracted the attention of researcher. Thus, the works in this field started to appear from 2017 and four distinct studies were published by: Rotavera et al. [18], Chen et al. [19], Telfah et al. [20] and Davies et al. [21]. Different experimental methods were used during these works: multiplexed photoionization mass spectrometry, infrared laser absorption spectroscopy and cavity ring-down spectroscopy. After determining the branching fractions of chain-termination pathways for THP and cyclohexane at 10 and 1520 Torr from 500 to 700 K, Rotavera et al. [18] proved that these low-temperature channels are more favored in THP due to its oxygen atom, while this functional group promote the ring-opening of adjacent THP radicals with the increase of temperature. Chen et al. [19] measured the formation of OH and HO_2 radicals in the reactions of THP and cyclohexane derived radicals with O_2 at 20 Torr within a temperature range of 500–750 K, and showed the possibility of comparing the low-temperature oxidation behavior of such fuels even without studying their detailed chemistry. Telfah et al. [20] detected tetrahydropyranyl peroxy radicals and associated the absence of that adjacent to the ether group to the favored ring opening of the corresponding tetrahydropyranyl radical. Davies et al. [21] compared the photoionization spectra of ketohydroperoxides produced from THP and cyclohexane, and revealed that the presence of ether group reduces the formation of ketohydroperoxides in cyclic hydrocarbons. Based on the foregoing literature review covering the main research conducted on the low-temperature chemistry of THP, one can notice that there is no work published yet investigating this chemistry in detail.

The present study covers both low- and high-temperature reactivity of THP in their details. It involves the oxidation of such a fuel in a JSR at a pressure (p) of 10 atm and a residence time (τ) of 700 ms, under four different equivalence ratios (φ) and in a temperature (T) range of 480–1260 K. The experimental conditions studied in this work are shown in Table 1.

Table 1
Experimental conditions tested.

Condition	φ (-)	T (K)	p (atm)	τ (ms)	THP (%)	O_2 (%)	N_2 (%)
1	0.5	480–1200	10	700	0.100	1.400	98.500
2	1.0	570–1200	10	700	0.100	0.700	99.200
3	2.0	570–1250	10	700	0.100	0.350	99.550
4	4.0	570–1260	10	700	0.100	0.175	99.725

2. Experimental apparatus

All the experiments of this work were carried out in a fused silica jet-stirred reactor of 42 cm^3, settled inside a stainless-steel pressure resistant jacket and heated by an electrical oven performing experiments up to 1280 K. To measure continuously the temperature within the reactor, a Pt/Pt-Rh 10 % thermocouple was used. This thermocouple is located inside a thin wall fused silica tube to avoid any catalytic reactions that can occur on the metallic wires.

The initial fuel mole fraction was set at 1000 ppm for all experiments, along with a pressure of 10 atm and a constant residence time of 700 ms. A high dilution of the reactive mixtures by nitrogen was done to prevent high heat release and experiments were performed at temperatures ranging from 480 to 1260 K. The liquid fuel (THP > 98.0 % pure from TCI, CAS Number 142–68–7, boiling point: 88 °C) was initially introduced into a controlled evaporator-mixer (CEM), where it was atomized after being mixed with a constant flow of auxiliary nitrogen and vaporized by setting the temperature of CEM at 90 °C. To avoid any premature reactions, the vaporized fuel flow was brought to the reactor through a capillary tube apart from the oxygen flow, which was brought through a separated stream together with the primary nitrogen flow. Then, both reactants and diluent were injected inside the reactor by its four nozzles (having each an inner diameter of 1 mm), which provide stirring. Mass flowmeters were used to control the flow rates of the diluent and reactants.

In order to perform a detailed analysis of the reacting mixture, samples were taken from the reactor using a low-pressure sonic probe. Online analyses were done by directly transmitting the samples taken to a Fourier transform infrared (FTIR) spectrometer via a heated line. FTIR was used to mainly quantify H_2O, CO, CO_2, and CH_2O. Samples were also stored at a low pressure of 80–90 mbar inside Pyrex bulbs for offline analyses using three different gas chromatographs (GC). Two of them are each coupled with a flame ionization detector (FID) and a mass spectrometer (MS), but are equipped with different columns: one has a DB624 column used to quantify oxygenated compounds while the second has a CP-Al_2O_3/KCl column used to quantify hydrocarbons. The identification of the products was done by GC/MS on a Shimadzu GC 2010 Plus, with electron impact (70 eV) as the ionization mode. The third GC is coupled with a thermal conductivity detector (TCD) and equipped with a CP-CarboPLOT P7 column, and it is used to measure both oxygen and hydrogen. The carbon balance was found to be typically within an uncertainty range of ±10–15 % for each sample.

3. Kinetic modeling

JSR simulations were carried out with the software CHEMKIN-PRO [22] using the Perfectly Stirred Reactor (PSR) code. The plug flow reactor (PLUG) and SENKIN modules were used to perform simulations in tubular flow reactor and shock tube respectively. The mechanism used for these simulations is based on the C_0–C_6 model developed previously by our team [23], including the detailed chemistry for various compounds such as alcohols, aldehydes and hydrocarbons. A new submechanism of THP oxidation was developed in this work covering both its low- and high-temperature reactivity. In this submechanism, the rate constants of the newly added reactions were adopted from literature by analogy to similar reactions already studied,

as detailed in the coming subsections. Thermodynamic data for the new species and radicals added to build the fuel submechanism resulted from calculations performed by RMG [24,25] and based on the group additivity method. The proposed mechanism is available in the supplementary material along with the corresponding thermochemical data.

3.1. High-temperature chemistry

Initiation reactions of fuel by C–H bond breaking were given in the direction of radical-radical recombination and a rate constant of 1×10^{14} s^{-1} was attributed to each of them. The two pericyclic reactions of THP (cy(occccc)) studied by Lizardo-Huerta et al. [26] were considered in our work: the isomerization forming an alcohol (pent4en1ol) and the H_2 elimination yielding a cyclic biradical (cy(ocjccccj)). This biradical will then undergo different pathways adopted from the work of Verdicchio et al. [27], who studied the analog biradical derived from tetrahydrofuran, while the sub-mechanism for pent4en1ol was taken from our previous work [28]. The rate constants for the ring-opening by the C–O and C–C bonds scission yielding n-pentanal (nc4h9cho) and unsaturated ethers (c4h7och3 and c3h7oc2h3) were estimated by analogy with the ring-opening of cyclohexane (CHX) from the work of Sirjean et al. [29]. While only one ring-opening is possible in the case of CHX, three different ring-opening reactions are possible in the case of THP due to the existence of three distinct bonds: C–O, C–C in β-position of ether group and C–C in its γ-position. Thus, the pre-exponential factor to be used for each THP ring-opening reaction was taken equal to that used for CHX divided by 3. To account for the presence of the oxygen atom in the ring of THP, the activation energy was reduced by 7 kcal/mol for the C–O bond scission and by 3.5 kcal/mol for the scission of the C–C bond in the β-position of the oxygen group. The effect of this oxygen on the C–C bond at the γ-position was assumed to be negligible and so the activation energy was considered without any alteration. The rate constants for the decomposition reactions of THP producing an aldehyde and an alkene were adopted by analogy to those of tetrahydrofuran (THF) as follows:

- For THP decomposition into formaldehyde and 1-butene, the rate constant was selected similarly to that of THF decomposition into formaldehyde and propene estimated by Verdicchio et al. [27].
- For THP decomposition either into acetaldehyde and propene or into propanal and ethylene, the rate constant was considered to be the same as that used by Fenard et al. [30] for THF decomposition into acetaldehyde and ethylene.

Although all the aforementioned unimolecular reactions of THP have a negligible effect under the oxidation conditions studied in this work, they were incorporated in our mechanism in order to simulate pyrolysis speciation data from the literature later in this article.

Rate constants for bimolecular initiation reactions by O_2 and for reactions of hydrogen abstraction from fuel were estimated based on analogies with di-n-propyl ether or THF for the alpha C–H site and with CHX for the beta and gamma C–H sites, as follows:

- For the α-site, the rate constants of bimolecular initiation by O_2 and of hydrogen abstraction reactions by OH, HO_2, O, CH_3, CH_3O_2 and C_2H_5 radicals were taken from Serinyel et al. [5] while the H-abstraction reactions by H, HCO, CH_2OH, and CH_3O were adopted from Fenard et al. [30].
- For the β- and γ-sites, rate constants were taken either from Zou et al. [31] or from Serinyel et al. [32] and were divided by 3 and 6 respectively. This is due to the fact that there are four equivalent C–H bonds in the β-site but only two in the γ-site, while twelve equivalent C–H bonds exist in CHX.

A correction was applied only for the H-abstraction reactions by OH radicals and H atoms; their pre-exponential factors were decreased by 50 %. This correction was made in order to have the best possible representation for the present experimental data by our model while keeping good estimations for the rate constants of these reactions; i.e., within the ranges expected for them based on relevant analogies done (see the supplementary material).

To determine the rate constants for the β-scission reactions of fuel radicals, accompanied by ring-opening, analogies were made with THF [30] and CHX [31] radicals. New β-scission reactions were then incorporated to account for the consumption of the newly formed radicals resulting from the decomposition of fuel radicals.

3.2. Low-temperature chemistry

Rate constants for addition reactions of fuel radicals (R) to molecular oxygen (O_2) forming RO_2 radicals were taken from the work of Goldsmith et al. [33]. Same rate constants were also attributed to the addition reactions of QOOH radicals to O_2, but they were divided by 2 to take into account the largeness of QOOH compared to R radicals. In fact, the presence of –OOH group could have a steric effect on QOOH, making it more difficult for this radical to collide successfully with O_2 (i.e., in an orientation that leads to a reaction) and thus reducing the pre-exponential factor in the rate constant of such a reaction.

For the reactions of R and O_2 producing dihydropyrans and HO_2, the rate constant was brought from DeSain et al. [34] with a reduction of 50 %. Only in the case of the fuel radical at the γ-position of the oxygen atom, the pre-exponential factor was then multiplied by 2 to take into consideration the four equivalent C–H bonds present in the β-position of this radical.

The rate constants for the isomerization of RO_2 to QOOH and their decomposition (both RO_2 and QOOH) to dihydropyrans and HO_2, as well as for the formation of cyclic ethers and ketohydroperoxides were adopted from Villano et al. [35,36] in the same manner considered previously for di-n-butyl ether [7]:

- For RO_2 isomerization to QOOH radicals, the activation energy proposed by the authors was reduced by 3 kcal.mol^{-1} only when the H atom to be transferred was at the α-position of the ether group.
- The rate constants for RO_2/QOOH decomposition and cyclic ether formation were considered without any alteration.
- The activation energy of ketohydroperoxides formation was reduced by 3 kcal.mol^{-1} when the carbonyl group is formed on the α-position of the ether group to take into account the effect of the two oxygenated groups (hydroperoxy and ether groups) on the C–H bond dissociation energy.

To account for the four equivalent C–H bonds present in the α- and β-positions of the ether group, the pre-exponential factor of RO_2 isomerization and decomposition reactions was multiplied by 2 when the peroxy group is at the γ-position.

After their formation, cyclic ethers were consumed through H-abstraction reactions by OH, H, and HO_2 radicals. The rate constants of these reactions were adopted from our previous work [5].

Finally, for the reactions of ketohydroperoxide decomposition, various values of rate constants could be found in the literature. Cai et al. [37] used a rate constant of $2.0 \times 10^{16} \times \exp(-35{,}000/RT)$ s^{-1}, which is much higher than that usually considered for this type of reaction, coming from the experimental study of Sahetchian et al. [38] ($4.0 \times 10^{15} \times \exp(-43{,}000/RT)$ s^{-1}). A slightly different activation energy or pre-exponential factor are also sometimes used, like in the study of Vasudevan et al. [39] ($2.5 \times 10^{15} \times \exp(-43{,}000/RT)$ s^{-1}). These reactions mainly depend on the fragility of the O–OH bond, which rapidly breaks and then the formed radical decomposes fast into chain branching fragments. The rate constant used for ketohydroperoxide decomposition in the present mechanism is set to $1.0 \times 10^{15} \times \exp(-43{,}000/RT)$ s^{-1}, showing the best prediction for the low-temperature experimental data obtained.

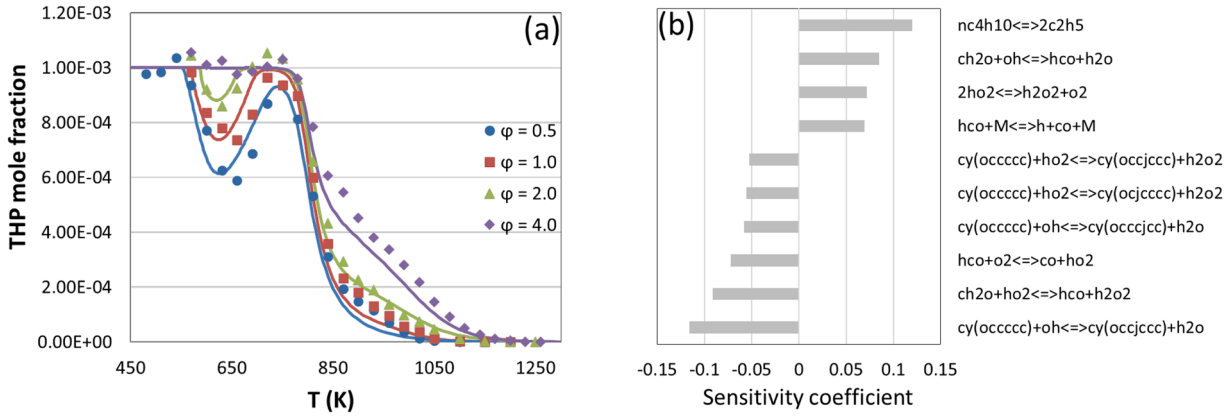

Fig. 1. Experimental (symbols) and computed (lines) mole fraction profiles of THP for all studied mixtures (a) and sensitivity analysis on THP performed with the present mechanism for the rich mixture ($\varphi = 4$) at 900 K (b).

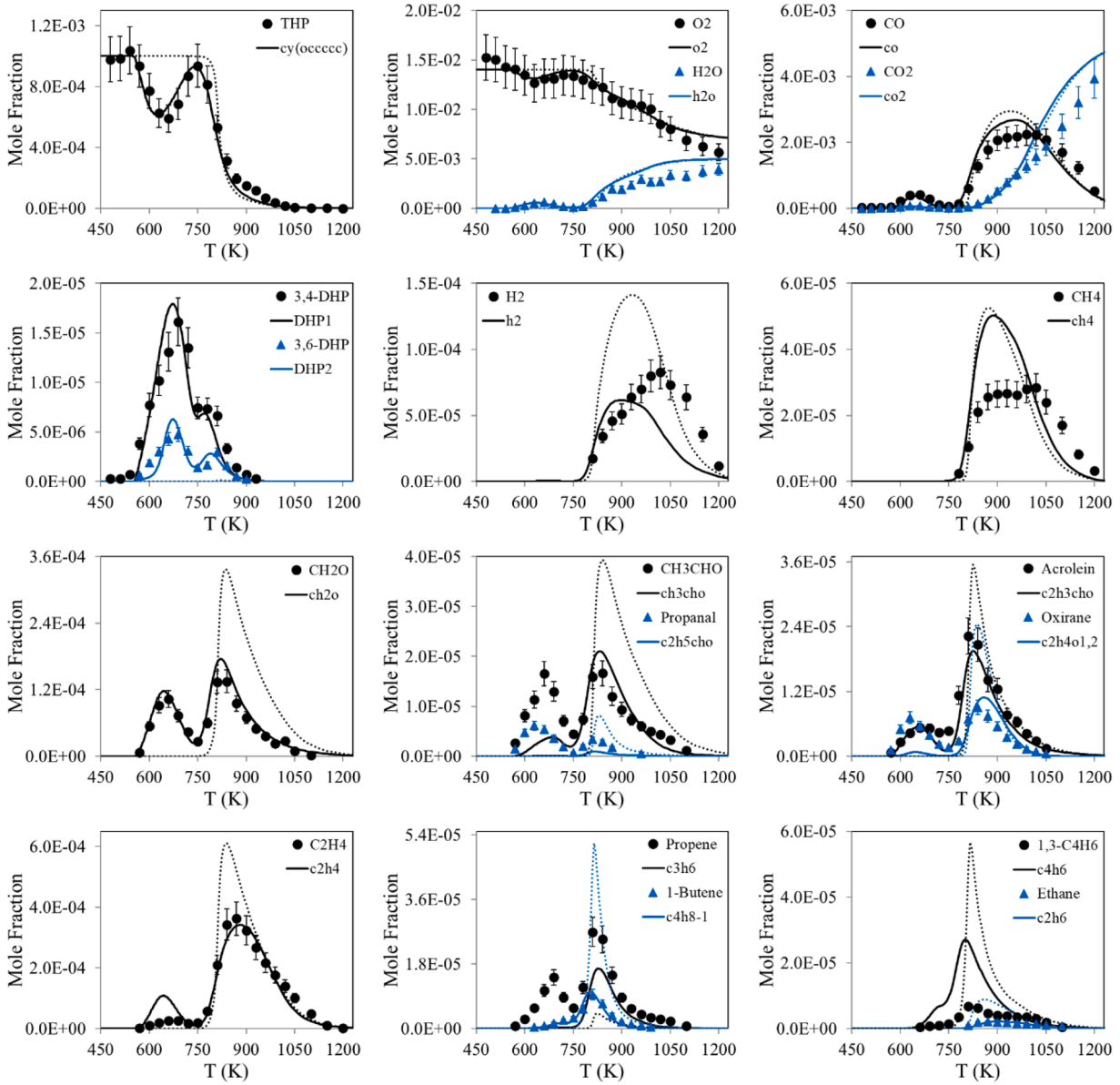

Fig. 2. Experimental (symbols) and computed (lines) mole fraction profiles obtained from the oxidation of THP in a JSR at $\varphi = 0.5$, $p = 10$ atm and $\tau = 0.7$ s. Solid lines: this work; dotted lines: Tran et al. [16] (designed only for high-temperature reactivity).

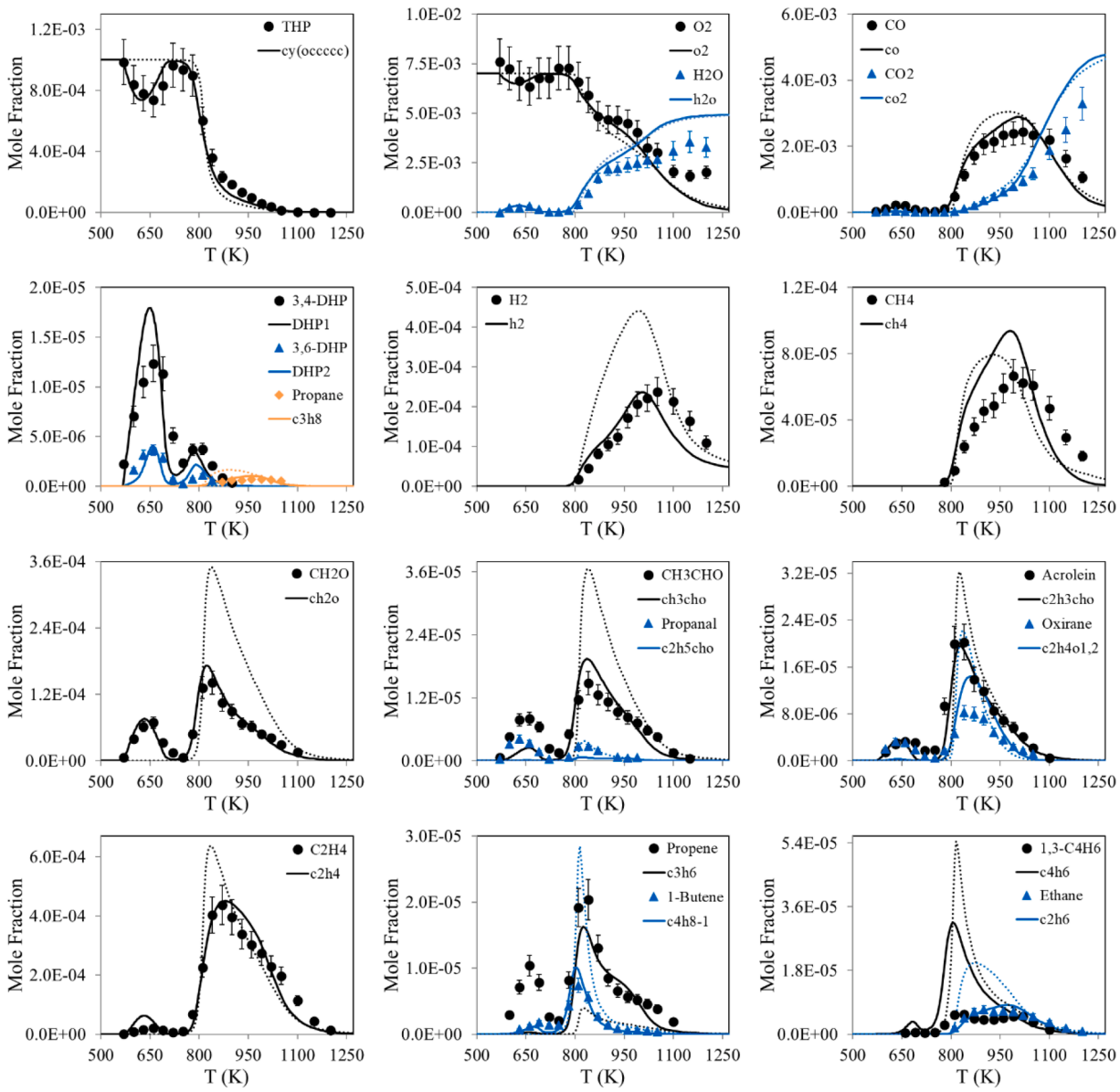

Fig. 3. Experimental (symbols) and computed (lines) mole fraction profiles obtained from the oxidation of THP in a JSR at $\varphi = 1$, $p = 10$ atm and $\tau = 0.7$ s. Solid lines: this work; dotted lines: Tran et al. [16] (designed only for high-temperature reactivity).

4. Results and discussion

As shown in Fig. 1a, THP exhibits a low-temperature reactivity that starts at about 570 K under the lean condition ($\varphi = 0.5$). When the equivalence ratio increases, this reactivity is slightly shifted toward higher temperatures and it becomes less pronounced to almost disappear at $\varphi = 4$. Then, a negative-temperature coefficient (NTC) region is observed between 630 and 750 K. This NTC zone is followed by the high-temperature reactivity at the end of which THP is totally consumed.

For the mixture with $\varphi = 4$, one can notice a significant drop in the high-temperature reactivity of the fuel, compared to those shown at the lower equivalence ratios. A sensitivity analysis (Fig. 1b) performed with the present mechanism at $\varphi = 4$ and $T = 900$ K highlights the importance of the recombination of ethyl radicals into n-butane under such conditions. In fact, this reaction appears here as the most positive-sensitive reaction with respect to the fuel (inhibiting its overall reactivity). This reaction was also found previously to be the most inhibiting reaction at pyrolysis conditions (1053 K and 170 kPa) [17].

In the figures (Figs. 2–5), the mole fraction profiles of the different species detected are illustrated along with simulations done by the present mechanism as well as by that of Tran et al. [17] covering only the high-temperature oxidation of THP. A representative 15 % uncertainty bar is added to experimental profiles. Apart from CO, CO_2 and H_2O, the most important oxygenated product observed during the low-temperature reactivity of THP was formaldehyde, which is a typical marker of low-temperature reactivity for many fuels. Other oxygenated products were also quantified: acetaldehyde, propanal, acrolein, oxirane and the two possible dihydropyrans (3,4- and 3,6-dihydro-2H-pyran) derived from THP. All these species were observed during both low- and high-temperature oxidation. The main hydrocarbon species quantified in this work was ethylene, followed by methane, ethane, propene, 1-butene and 1,3-butadiene. Traces of propane also appeared with the increase of equivalence ratio. In addition, under the rich conditions, a considerable formation of acetylene could be clearly observed at high temperatures. At these temperatures, the formation of benzene along with traces of propyne and allene was as well detected with the $\varphi = 4$ mixture.

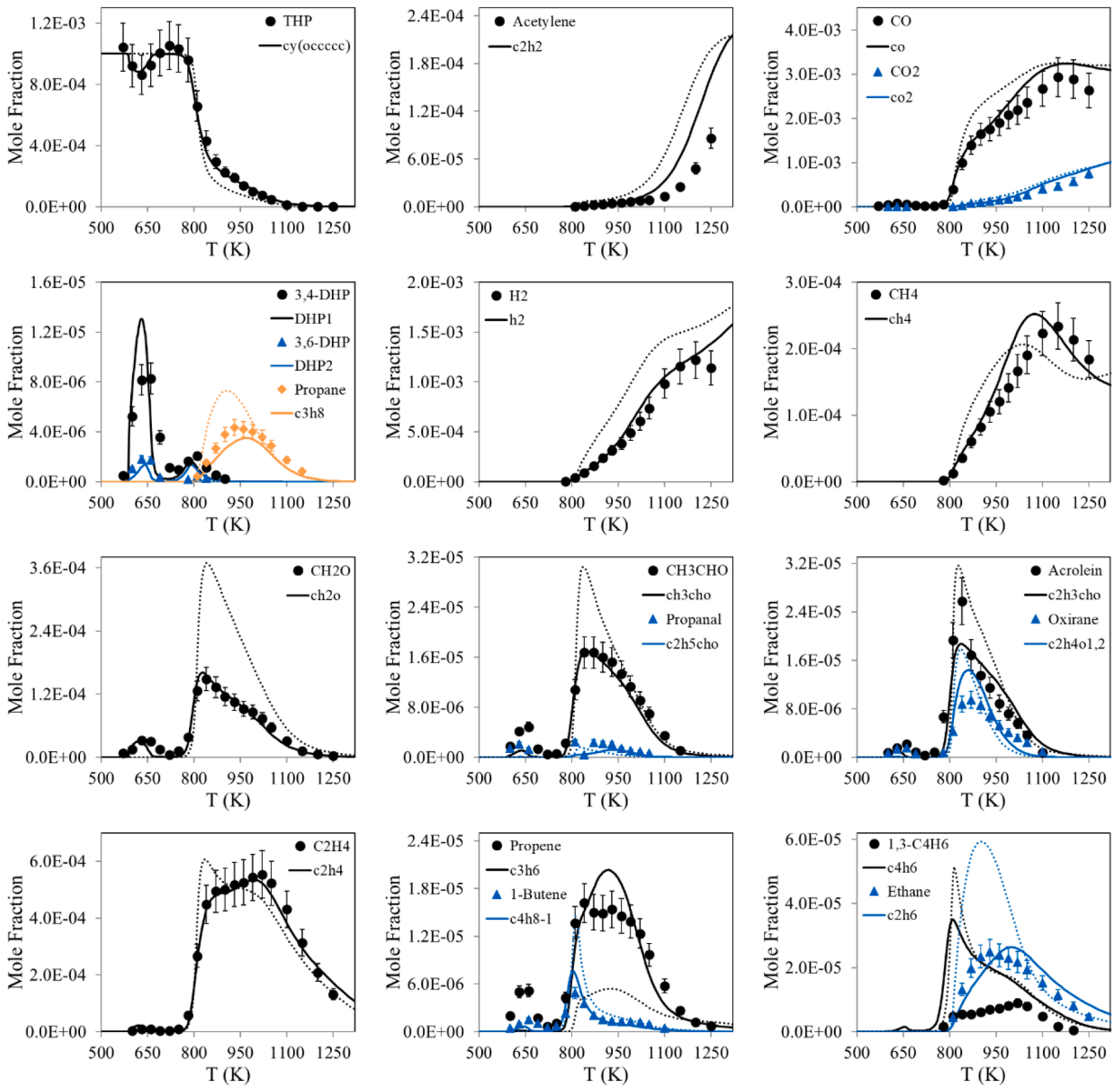

Fig. 4. Experimental (symbols) and computed (lines) mole fraction profiles obtained from the oxidation of THP in a JSR at $\varphi = 2$, $p = 10$ atm and $\tau = 0.7$ s. Solid lines: this work; dotted lines: Tran et al. [16] (designed only for high-temperature reactivity).

The present mechanism predicts well the mole fraction profiles of the fuel under the four conditions tested although it shows a slight underprediction between 840 and 990 K for the lean and stoichiometric mixtures. Generally speaking, this mechanism also has a good performance for representing the mole fractions of the different species obtained despite the presence of some discrepancies. Indeed, these discrepancies arise from the uncertainties on the rate parameters used for the main reactions of the fuel submechanism, which are not directly calculated or measured for THP itself but rather estimated based on analogies with similar fuels. Moreover, thermochemical data have a crucial importance, especially those of the low-temperature radicals (RO_2, QOOH and OOQOOH). These parameters have to be as precise as possible in addition to the kinetics. The use of group additivity method may encounter limitations when dealing with such large and complex radicals. Getting more accurate kinetic data is substantial for understanding the detailed chemistry of THP, but the effect of the uncertainties on thermochemistry should not be neglected.

On the other hand, the mechanism of Tran et al. [17] tends to significantly overpredict the production of most species for the different studied mixtures. Also, it highly underpredicts the mole fractions of some species: propene and dihydropyrans; the formation of benzene was as well underestimated ($\varphi = 4$). Both mechanisms underpredict the fuel mole fraction between 840 and 990 K for both lean and stoichiometric mixtures. However, this underprediction is more pronounced in the case of Tran mechanism at all conditions and it becomes more important and seen within a wider temperature window when the mixture becomes rich (between 800 and 1100 K at $\varphi = 4$).

Both mechanisms highly overpredict the mole fraction of 1,3-butadiene for all studied conditions at high temperatures starting from 750 K. Nevertheless, a better prediction can be noticed for the mole fraction of this species in the end of its final consumption; beyond a certain value of temperature which seems to differ from a condition to another, higher than 950 K in any case. The reaction pathways leading to the formation of 1,3-butadiene at high temperatures are revealed in the next section.

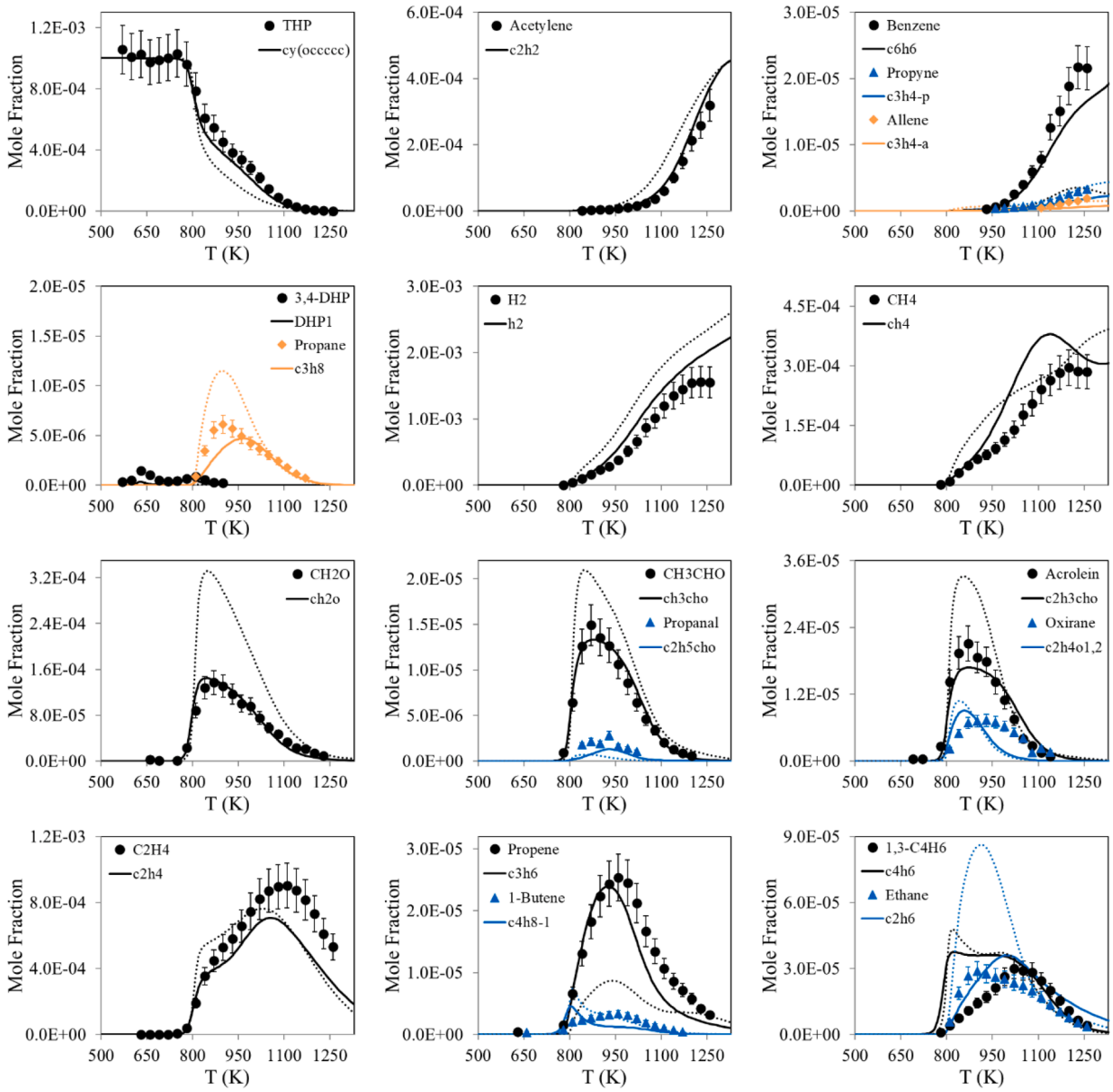

Fig. 5. Experimental (symbols) and computed (lines) mole fraction profiles obtained from the oxidation of THP in a JSR at $\varphi = 4$, $p = 10$ atm and $\tau = 0.7$ s. Solid lines: this work; dotted lines: Tran et al. [16] (designed only for high-temperature reactivity).

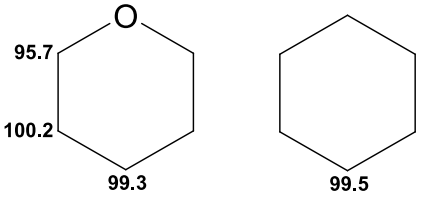

Fig. 6. C–H bond dissociation energies of THP and CHX calculated with RMG [20,21].

Finally, we should mention that although it represents well the major oxygenated species (formaldehyde) obtained during the low-temperature oxidation of THP, our model failed in predicting the formation of minor products (acetaldehyde, oxirane, propanal and propene) during such a reactivity and further investigation is still required to propose a mechanistic explanation for their formation at low temperatures.

5. Reaction pathways

THP can form three distinct radicals: α-radical (cy(ocjcccc)), β-radical (cy(occjccc)) and γ-radical (cy(occcjcc)). C–H bond dissociation energies (BDEs) for THP were calculated using RMG [24,25] and are presented in Fig. 6. The alpha C–H bond is the weakest and therefore the corresponding fuel α-radical is the most favored one. Also, note that the beta and gamma C–H bonds in THP have BDE values which are close to that of the C–H bond in CHX, confirming the choice of analogy.

Fig. 7 shows the main reaction pathways for the low-temperature oxidation of THP with the percentages evaluated at $\varphi = 0.5$ and $T = 580$ K. As it can be clearly seen, the fuel is consumed through H-abstraction reactions by OH radicals to form its three primary radicals. These radicals mainly undergo an addition to molecular oxygen forming their corresponding RO_2 radicals. Then, RO_2 radicals mostly go through isomerization (internal hydrogen transfer) to produce QOOH radicals. In their turn, the QOOH radicals primarily undergo a second addition to O_2 followed by another isomerization to finally give ketohydroperoxides after an OH elimination. Due to the rapid breakage of its weak O–OH

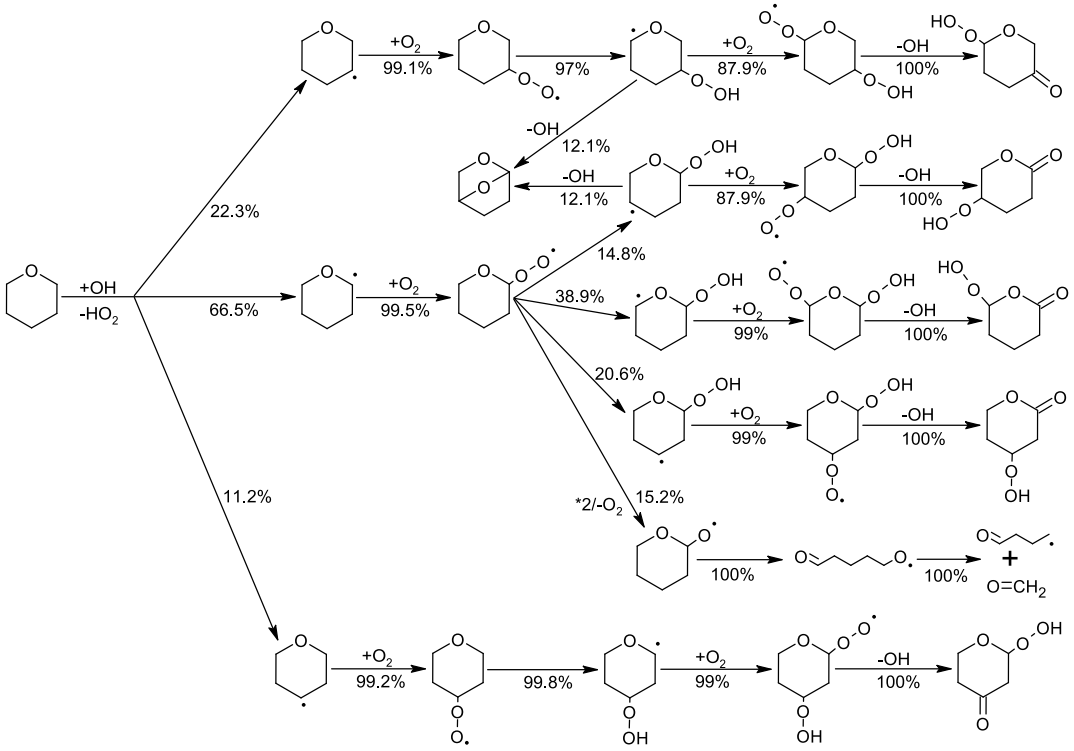

Fig. 7. Main reaction pathways shown by our model for the mixture ($\varphi = 0.5$) at 580 K.

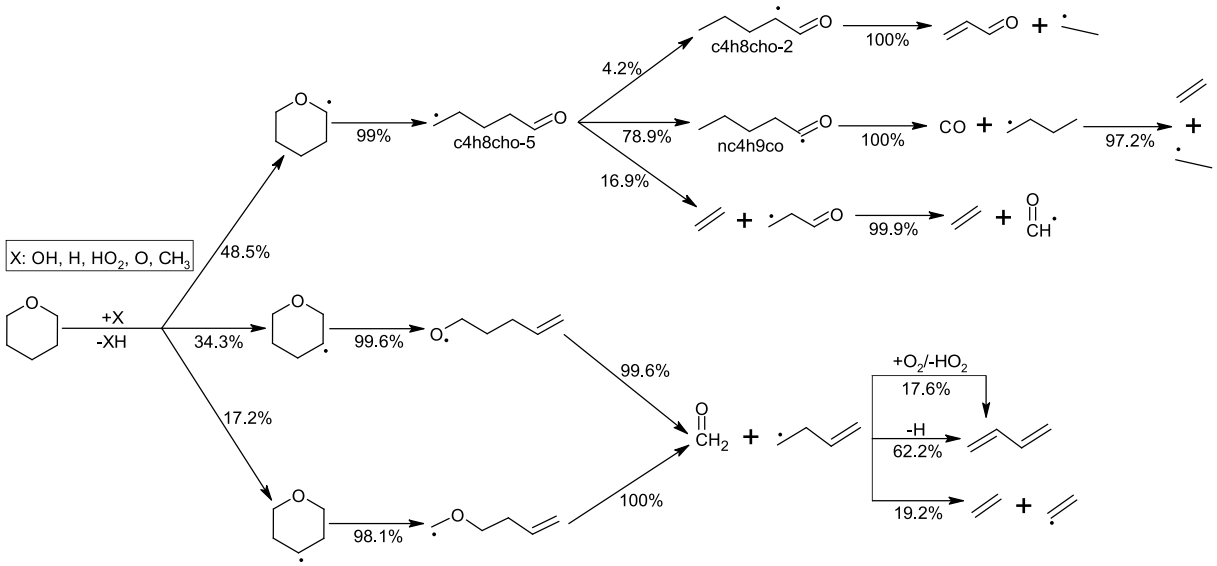

Fig. 8. Main reaction pathways shown by our model for the mixture ($\varphi = 4$) at 900 K.

bond, a ketohydroperoxide quickly decomposes into chain branching fragments and an OH radical, promoting the overall reactivity.

Another reaction pathway analysis was performed with our model at $\varphi = 4$ and $T = 900$ K (Fig. 8). Again, the fuel is consumed through H-abstraction reactions mostly by OH radicals but also by H, HO_2, O and CH_3. At such conditions, the fuel radicals dominantly undergo a β-scission accompanied by ring-opening. In their turn, the newly obtained radicals undergo another β-scission but may also go through isomerization. However, such an isomerization reaction should be favored enough to compete with the β-scission, like in the case of the primary pentanal radical (c4h8cho-5) formed from the ring-opening of the fuel α-radical. In fact, c4h8cho-5 can undergo a favorable isomerization via an internal H-transfer, which simultaneously involves a six-membered transition state and a transfer of an aldehydic H to give another pentanal radical (nc4h9co). The radical c4h8cho-5 can also go through an internal H-transfer with a five-membered transition state leading to the formation of a secondary pentanal radical (c4h8cho-2), but this isomerization is much less favored (only 4.2 % of c4h8cho-5 followed this pathway). We can see that the most important reaction pathway of the fuel α-radical is mainly ended by forming ethyl radicals, confirming the crucial inhibiting role of the recombination reaction of such radicals (chain termination) on the global reactivity. Furthermore, we can identify the high-temperature pathways that lead to the formation of 1,3-butadiene. This species is the dominant product obtained from the

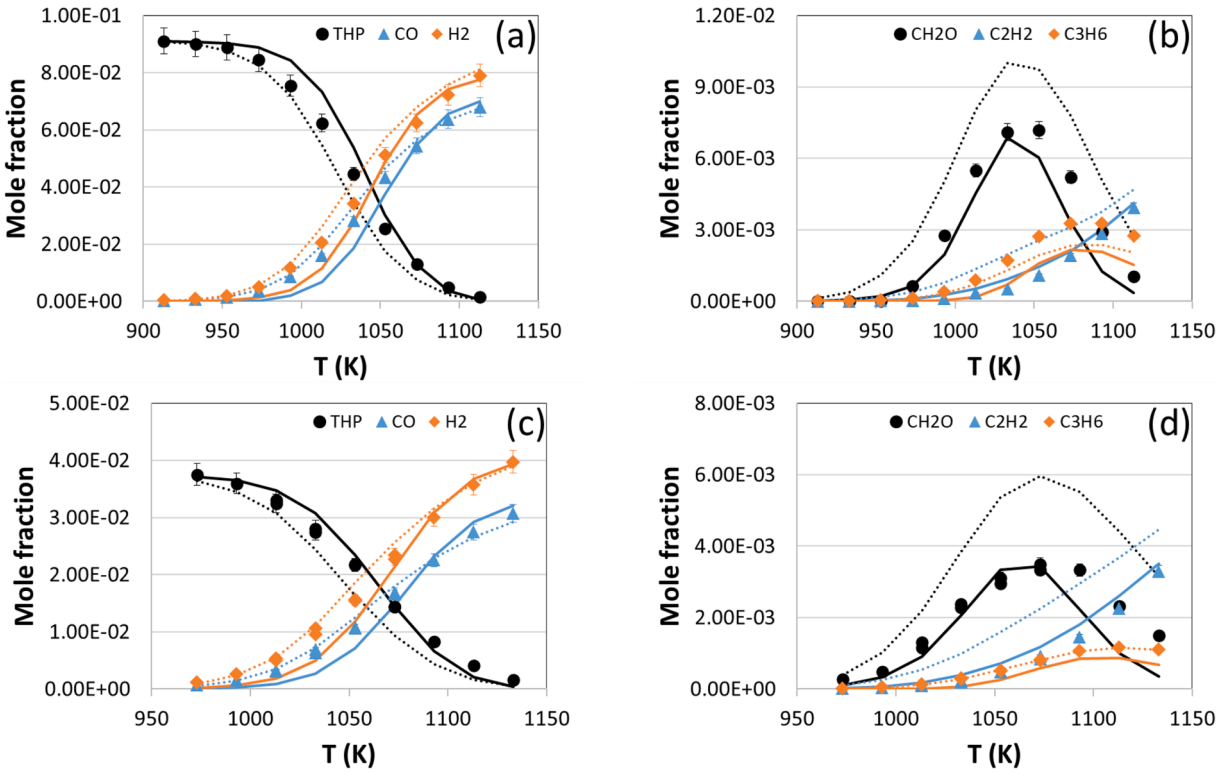

Fig. 9. Mole fraction profiles of fuel and some species obtained during THP pyrolysis in a tubular flow reactor at 170 kPa using two different N_2 dilution factors of: 90 % (a,b) and 96 % (c,d). Symbols: experiments [16]; lines: simulations (solid: this work, dotted: Tran et al. [16]).

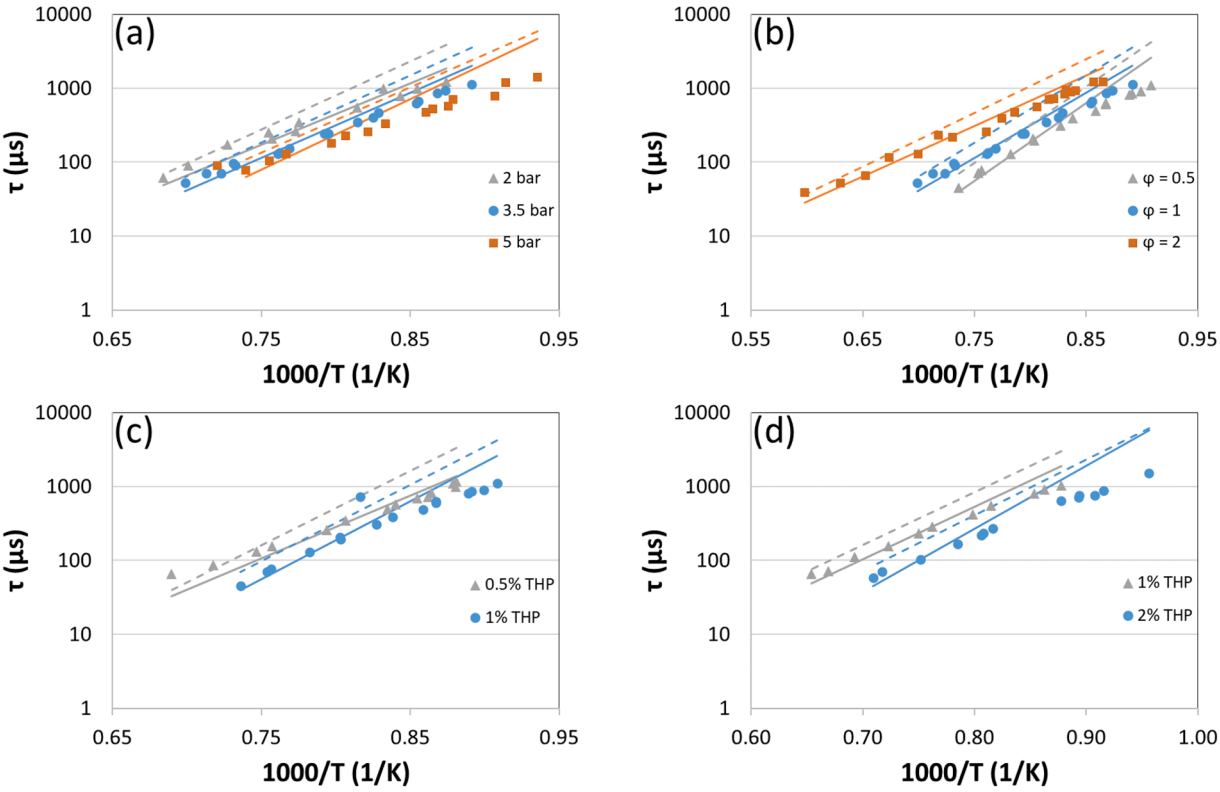

Fig. 10. Ignition delay times of THP/O_2/Ar auto-ignition in a shock tube at: three different pressures under $\varphi = 1$ and 1 % THP (a), three distinct equivalence ratios under 3.5 bar and 0.5 % THP (b) and two various fuel concentrations either under 3.5 bar and $\varphi = 0.5$ (c) or under 5 bar and $\varphi = 2$ (d). Symbols: experiments [14]; lines: simulations (solid: this work, dashed: Tran et al. [16]).

pathways followed by both β- and γ-radicals of fuel. Indeed, after two consecutive β-scission reactions, these radicals give formaldehyde and the primary radical of 1-butene. The 1,3-butadiene is then produced from this radical through a direct H loss, and also via an H-transfer to O_2 but to a lesser extent. Thus, it seems that the over-prediction of 1,3-butadiene by our model is due to an overestimation of the rate constants adopted for the aforementioned β-scission reactions.

6. Further validation

The present mechanism was further tested on other types of experimental results previously published in the literature. These results include plug flow reactor (PFR) data from the work of Tran et al. [17] (Fig. 9) and ignition delay times (IDT) from the work of Dagaut et al. [15] (Fig. 10). The general tendency of these data is well represented by our model.

For the mole fraction profiles obtained from the pyrolysis of THP in a PFR, our model predicts well the fuel conversion for the mixture of THP with 96 % N_2 (Fig. 9c), but this conversion is underestimated between 953 and 1053 K for the mixture of THP with 90 % N_2 (Fig. 9a). The model also shows good agreement with the mole fractions of some major (CO and H_2) and relatively minor (CH_2O, C_2H_2 and C_3H_6) species (Fig. 9b and d) obtained during such a pyrolysis despite the presence of some discrepancies. The present mechanism was also compared to that developed by Tran et al. [17] to simulate such data. This latter mechanism overpredicts the fuel reactivity within the temperature range 993–1093 K for the mixture of 90 % N_2 and along the entire temperature range tested for the second mixture. This overestimation of reactivity resulted in an overprediction of CH_2O and C_2H_2 formation. However, the three other computed products are well represented by this model.

For the auto-ignition of THP in a shock tube, the present mechanism predicts well the increase of reactivity seen either with increasing the pressure (Fig. 10a), decreasing the equivalence ratio (Fig. 10b) or increasing the initial fuel concentration (Fig. 10c and d). It also shows a very good performance in predicting the IDT values, although it tends to overpredict some of them with the increase of pressure, the decrease of equivalence ratio and/or the increase of initial THP concentration. Indeed, this overprediction is only seen at the lowest temperatures tested, especially under the highest pressure studied (5 bar), but then it becomes less pronounced when the temperature increases to totally disappear beyond a certain value of temperature. On the other hand, Tran mechanism overestimates the IDT under the different conditions tested but this overestimation decreases as well with temperature.

7. Conclusion

The oxidation of THP was studied in a jet-stirred reactor at a high pressure using an experimental and modeling approach. This study includes the high-temperature reactivity of THP but also its low-temperature oxidation, previously unexplored. In fact, THP exhibits a low-temperature reactivity and an NTC region similar to those observed for alkanes. A detailed kinetic model was developed in order to understand the oxidation patterns of THP. This model generally shows a good performance in predicting the experimental data obtained, and yields better simulations when compared to the mechanism of Tran et al. [17] designed only for the high-temperature reactivity of THP. However, some discrepancies exist due to the uncertainties on the rate constants and thermochemical data adopted in this work. These uncertainties could be removed using advanced theoretical calculations.

For the rich mixture ($\varphi = 4$), the fuel showed a significant drop in its high-temperature reactivity. A sensitivity analysis proved that this reactivity drop was observed due to a crucial termination reaction occurring under such conditions, the recombination reaction of ethyl radicals. The importance of these radicals was also confirmed after performing a reaction pathway analysis at the same conditions. This analysis was used as well to identify the pathways contributing to the formation of 1,3-butadiene in an attempt to find the essential roots causing its over-prediction by the present mechanism.

Finally, some PFR and IDT data taken from the literature were used to further validate the present mechanism, which shows again better agreement with the experimental results when compared to Tran mechanism. Nevertheless, more data (including laminar flame speeds) are still needed in order to achieve this validation and to fully understand the kinetic behavior of THP. The current work could be extended in the future to involve the oxidation of THP at the atmospheric pressure but more JSR experiments are first required.

CRediT authorship contribution statement

Bakr Hoblos: Writing – original draft, Visualization, Methodology, Investigation. **Zeynep Serinyel:** Writing – review & editing, Supervision, Methodology, Conceptualization. **Guillaume Dayma:** Writing – review & editing, Methodology, Conceptualization. **Philippe Dagaut:** Writing – review & editing, Validation, Methodology.

Declaration of competing interests

The authors declare that they have no known competing financial interests or personal relationships that could have appeared to influence the work reported in this paper.

Acknowledgements

BH thanks the French Ministry of Education and Scientific Research for a PhD grant. Support from the CAPRYSSES project (ANR-11-LABX-006–01) funded by ANR through the PIA (Programme d'Investissement d'Avenir) and from the KINOXET project (ANR-20-CE05–0017) is also gratefully acknowledged.

Supplementary materials

Supplementary material associated with this article can be found, in the online version, at doi:10.1016/j.combustflame.2024.113642.

References

[1] P. Dagaut, C. Daly, J.M. Simmie, M. Cathonnet, The oxidation and ignition of dimethylether from low to high temperature (500–1600 K): experiments and kinetic modeling, Symp. (Int.) Combust. 27 (1998) 361–369.
[2] C. Yan, H. Zhao, Z. Wang, G. Song, Y. Lin, C.R. Mulvihill, A.W. Jasper, S. J. Klippenstein, Y. Ju, Low- and intermediate-temperature oxidation of dimethyl ether up to 100 atm in a supercritical pressure jet-stirred reactor, Combust. Flame 243 (2022) 112059.
[3] Z. Serinyel, M. Lailliau, S. Thion, G. Dayma, P. Dagaut, An experimental chemical kinetic study of the oxidation of diethyl ether in a jet-stirred reactor and comprehensive modeling, Combust. Flame 193 (2018) 453–462.
[4] L.-S. Tran, O. Herbinet, Y. Li, J. Wullenkord, M. Zeng, E. Bräuer, F. Qi, K. Kohse-Höinghaus, F. Battin-Leclerc, Low-temperature gas-phase oxidation of diethyl ether: fuel reactivity and fuel-specific products, Proc. Combust. Inst. 37 (2019) 511–519.
[5] Z. Serinyel, M. Lailliau, G. Dayma, P. Dagaut, A high pressure oxidation study of di-n-propyl ether, Fuel 263 (2020) 116554.
[6] N. Belhadj, R. Benoit, P. Dagaut, M. Lailliau, Z. Serinyel, G. Dayma, Oxidation of di-n-propyl ether: characterization of low-temperature products, Proc. Combust. Inst. 38 (2021) 337–344.
[7] S. Thion, C. Togbé, Z. Serinyel, G. Dayma, P. Dagaut, A chemical kinetic study of the oxidation of dibutyl-ether in a jet-stirred reactor, Combust. Flame 185 (2017) 4–15.
[8] N. Belhadj, R. Benoit, P. Dagaut, M. Lailliau, Z. Serinyel, G. Dayma, F. Khaled, B. Moreau, F. Foucher, Oxidation of di-n-butyl ether: experimental characterization of low-temperature products in JSR and RCM, Combust. Flame 222 (2020) 133–144.
[9] B. Rotavera, C.A. Taatjes, Influence of functional groups on low-temperature combustion chemistry of biofuels, Prog. Energy Combust. Sci. 86 (2021) 100925.
[10] L.-S. Tran, O. Herbinet, H.-H. Carstensen, F. Battin-Leclerc, Chemical kinetics of cyclic ethers in combustion, Prog. Energy Combust. Sci. 92 (2022) 101019.
[11] A. Osmont, L. Catoire, P.Escot Bocanegra, I. Gökalp, B. Thollas, J.A. Kozinski, Second generation biofuels: thermochemistry of glucose and fructose, Combust. Flame 157 (2010) 1230–1234.

[12] R.M. West, E.L. Kunkes, D.A. Simonetti, J.A. Dumesic, Catalytic conversion of biomass-derived carbohydrates to fuels and chemicals by formation and upgrading of mono-functional hydrocarbon intermediates, Catal. Today 147 (2009) 115–125.
[13] O. Herbinet, F. Battin-Leclerc, Progress in understanding low-temperature organic compound oxidation using a jet-stirred reactor, Int. J. Chem. Kinet. 46 (2014) 619–639.
[14] W.R. Leppard, The autoignition chemistries of octane-enhancing ethers and cyclic ethers: a motored engine study, SAE Trans. 100 (1991) 589–604.
[15] P. Dagaut, M. McGuinness, J.M. Simmie, M. Cathonnet, The ignition and oxidation of tetrahydropyran: experiments and kinetic modeling, Combust. Sci. Technol. 129 (1997) 1–16.
[16] N.J. Labbe, V. Seshadri, T. Kasper, N. Hansen, P. Oßwald, P.R. Westmoreland, Flame chemistry of tetrahydropyran as a model heteroatomic biofuel, Proc. Combust. Inst. 34 (2013) 259–267.
[17] L.-S. Tran, R. De Bruycker, H.-H. Carstensen, P.-A. Glaude, F. Monge, M.U. Alzueta, R.C. Martin, F. Battin-Leclerc, K.M. Van Geem, G.B. Marin, Pyrolysis and combustion chemistry of tetrahydropyran: experimental and modeling study, Combust. Flame 162 (2015) 4283–4303.
[18] B. Rotavera, J.D. Savee, I.O. Antonov, R.L. Caravan, L. Sheps, D.L. Osborn, J. Zádor, C.A. Taatjes, Influence of oxygenation in cyclic hydrocarbons on chain-termination reactions from R + O2: tetrahydropyran and cyclohexane, Proc. Combust. Inst. 36 (2017) 597–606.
[19] M.-W. Chen, B. Rotavera, W. Chao, J. Zádor, C.A. Taatjes, Direct measurement of ȮH and HO2̇ formation in Ṙ + O2 reactions of cyclohexane and tetrahydropyran, Phys. Chem. Chem. Phys. 20 (2018) 10815–10825.
[20] H. Telfah, M.A. Reza, J. Alam, A.C. Paul, J. Liu, Direct observation of tetrahydrofuranyl and tetrahydropyranyl peroxy radicals via cavity ring-down spectroscopy, J. Phys. Chem. Lett. 9 (2018) 4475–4480.
[21] J.C. Davis, A.L. Koritzke, R.L. Caravan, I.O. Antonov, M.G. Christianson, A. C. Doner, D.L. Osborn, L. Sheps, C.A. Taatjes, B. Rotavera, Influence of the ether functional group on ketohydroperoxide formation in cyclic hydrocarbons: tetrahydropyran and cyclohexane, J. Phys. Chem. A 123 (2019) 3634–3646.
[22] ANSYS CHEMKIN-PRO 2022 R2, ANSYS Reaction Design: San Diego, 2022.
[23] Z. Serinyel, C. Togbé, G. Dayma, P. Dagaut, Experimental and modeling study of the oxidation of two branched aldehydes in a jet-stirred reactor: 2-methylbutanal and 3-methylbutanal, Energy Fuels 31 (2017) 3206–3218.
[24] M. Liu, A. Grinberg Dana, M.S. Johnson, M.J. Goldman, A. Jocher, A.M. Payne, C. A. Grambow, K. Han, N.W. Yee, E.J. Mazeau, K. Blondal, R.H. West, C. F. Goldsmith, W.H. Green, Reaction mechanism generator v3.0: advances in automatic mechanism generation, J. Chem. Inf. Model. 61 (2021) 2686–2696.
[25] M.S. Johnson, X. Dong, A. Grinberg Dana, Y. Chung, D.Jr. Farina, R.J. Gillis, M. Liu, N.W. Yee, K. Blondal, E. Mazeau, C.A. Grambow, A.M. Payne, K. A. Spiekermann, H.-W. Pang, C.F. Goldsmith, R.H. West, W.H. Green, RMG database for chemical property prediction, J. Chem. Inf. Model. 62 (2022) 4906–4915.
[26] J.-C. Lizardo-Huerta, B. Sirjean, P.-A. Glaude, R. Fournet, Pericyclic reactions in ether biofuels, Proc. Combust. Inst. 36 (2017) 569–576.
[27] M. Verdicchio, B. Sirjean, L.S. Tran, P.-A. Glaude, F. Battin-Leclerc, Unimolecular decomposition of tetrahydrofuran: carbene vs. diradical pathways, Proc. Combust. Inst. 35 (2015) 533–541.
[28] G. Dayma, Z. Serinyel, M. Carbonnier, J. Bai, Y. Zhu, C.-W. Zhou, A. Kéromnès, B. Lefort, L. Le Moyne, P. Dagaut, Oxidation of pentan-2-ol – part II: experimental and modeling study, Proc. Combust. Inst. 38 (2021) 833–841.
[29] B. Sirjean, P.A. Glaude, M.F. Ruiz-Lopez, R. Fournet, Detailed kinetic study of the ring opening of cycloalkanes by CBS-QB3 calculations, J. Phys. Chem. A 110 (2006) 12693–12704.
[30] Y. Fenard, A. Gil, G. Vanhove, H.-H. Carstensen, K.M. Van Geem, P. R. Westmoreland, O. Herbinet, F. Battin-Leclerc, A model of tetrahydrofuran low-temperature oxidation based on theoretically calculated rate constants, Combust. Flame 191 (2018) 252–269.
[31] J. Zou, H. Jin, D. Liu, X. Zhang, H. Su, J. Yang, A. Farooq, Y. Li, A comprehensive study on low-temperature oxidation chemistry of cyclohexane. II. Experimental and kinetic modeling investigation, Combust. Flame 235 (2022) 111550.
[32] Z. Serinyel, O. Herbinet, O. Frottier, P. Dirrenberger, V. Warth, P.A. Glaude, F. Battin-Leclerc, An experimental and modeling study of the low- and high-temperature oxidation of cyclohexane, Combust. Flame 160 (2013) 2319–2332.
[33] C.F. Goldsmith, W.H. Green, S.J. Klippenstein, Role of O2 + QOOH in low-temperature ignition of propane. 1. Temperature and pressure dependent rate coefficients, J. Phys. Chem. A 116 (2012) 3325–3346.
[34] J.D. DeSain, S.J. Klippenstein, J.A. Miller, C.A. Taatjes, Measurements, theory, and modeling of OH formation in Ethyl + O2 and Propyl + O2 reactions, J. Phys. Chem. A 107 (2003) 4415–4427.
[35] S.M. Villano, L.K. Huynh, H.-H. Carstensen, A.M. Dean, High-pressure rate rules for Alkyl + O2 reactions. 1. The dissociation, concerted elimination, and isomerization channels of the alkyl peroxy radical, J. Phys. Chem. A 115 (2011) 13425–13442.
[36] S.M. Villano, L.K. Huynh, H.-H. Carstensen, A.M. Dean, High-pressure rate rules for Alkyl + O2 Reactions. 2. The isomerization, cyclic ether formation, and β-scission reactions of hydroperoxy alkyl radicals, J. Phys. Chem. A 116 (2012) 5068–5089.
[37] L. Cai, A. Sudholt, D.J. Lee, F.N. Egolfopoulos, H. Pitsch, C.K. Westbrook, S. M. Sarathy, Chemical kinetic study of a novel lignocellulosic biofuel: di-n-butyl ether oxidation in a laminar flow reactor and flames, Combust. Flame 161 (2014) 798–809.
[38] K.A. Sahetchian, R. Rigny, J. Tardieu de Maleissye, L. Batt, M. Anwar Khan, S. Mathews, The pyrolysis of organic hydroperoxides (ROOH), Symp. (Int.) Combust. 24 (1992) 637–643.
[39] V. Vasudevan, D.F. Davidson, R.K. Hanson, Direct measurements of the reaction OH + CH2O → HCO + H2O at high temperatures, Int. J. Chem. Kinet. 37 (2005) 98–109.